

Probing electrodynamic properties of the edge states in a quantum Hall system by surface photovoltage spectroscopy

B. Karmakar,¹ G. H. Dohler,^{2,1} and B. M. A. Arora¹

¹Tata Institute of Fundamental Research, Mumbai, India

²University of Erlangen, Erlangen, Germany

(Dated: April 14, 2024)

An important question regarding the dissipation-less current carried by the edge states in a quantum Hall system is understanding the results of the electrodynamic interaction among the mobile electrons in the quantum mechanical limit under a magnetic field B . The interaction affects the transport parameters, the transverse electric field and the electron velocity. We have developed a new surface photovoltage spectroscopic technique to measure the parameters from the transition energies between the electron and heavy hole edge states. We observe that the measured electron velocity and transverse (Hall) electric field increase as $B^{1/2}$ and $B^{3/2}$ respectively.

PACS numbers: 73.43.-f, 07.60.R, 73.43.Fj

The dispersive edge states carry dissipation-less diamagnetic current^{1,2} along the boundary of a two-dimensional electron system (2DES) under a perpendicular magnetic field B . The current is carried one-dimensionally by the filled edge states in a sub-micron conducting-strip³, which lies next to a sub-micron depletion-strip^{4,5} of empty edge states at the boundary. Using single particle picture, Halperin¹ showed the formation of current carrying edge states in the quantum Hall (QH) system. But in a real system, interacting mobile (chiral motion) electrons are present in the conducting-strip. The mobile electrons generate Hall field, which modify the transverse confining (electrostatic) electric field⁶ and electro-chemical potential⁷ at the boundary of the 2DES. The modified transverse electric field determines the velocity of electrons and the energies of the edge states. Therefore, in the presence of a strong magnetic field, the electro-dynamically interacting mobile electrons in the edge states modify the physical parameters pertaining to the dissipation-less current. However, the B -dependences of the physical parameters viz. the electric field, the velocity of electrons and the energies⁸ of the edge states have neither been measured nor theoretically predicted. We have developed a surface photovoltage (SPV) spectroscopic⁹ technique with a new variation so as to probe the edge states distinctively from the Landau levels (LLs) in the interior of a QH system. Our SPV technique is naturally selective to measure the average transition energies between the electron and heavy hole edge states at the interface of conducting and depletion strips. From the transition energies, we explore the electric field and the velocity of the electrons in the edge states at the interface.

To perform the SPV experiments, in the narrow available range of energies (763–816 meV) from tunable diode laser sources, a suitable InP/In_{0.65}Ga_{0.35}As/InP modula-

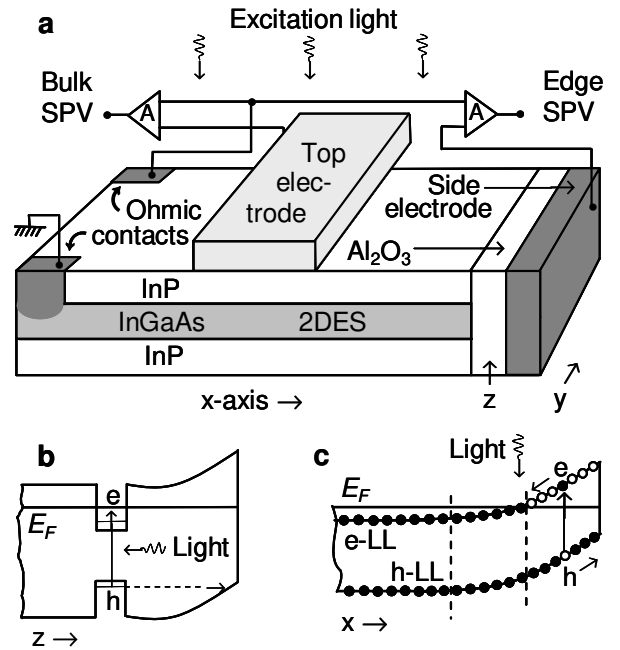


FIG. 1: a) Schematic device structure and measurement setup. 'A' is unity gain buffer-amplifier circuit. b) Schematic band diagram along the growth direction (z) to explain B-SPV signal generation. c) Schematic band diagram along the plane of the QW (x) towards the boundary to explain E-SPV signal generation. Electron and heavy hole LLs are labeled e-LL and h-LL respectively. Vertical dashed lines separate bulk-region, conducting-strip and depletion-strip successively.

tion doped quantum well (QW) sample is designed (Fig. 1a). The electron gas in the 2DES resides 400 Å below the top surface in the 90 Å thick InGaAs QW, has an electron density $n_s = 6.6 \times 10^{11} \text{ cm}^{-2}$ and a mobility $10^5 \text{ cm}^2/\text{V-s}$. The sample is excited from top (Fig. 1a) with unpolarized infrared light, chopped at 20 Hz carried with an optical fiber. Electron-hole pairs are generated by electronic transitions from the filled va-

Electronic address: karmakar@tifr.res.in

lence band to the empty conduction band states above the Fermi energy E_F in the QW (Fig. 1b). The bulk SPV (B-SPV) signal⁹ is generated by the tunnelling of holes from the QW to the top surface (Fig. 1b) and is measured with excitation power density 1 W/cm^2 (after attenuation) between an ohmic contact and the top indium-tin-oxide coated glass electrode (Fig. 1a) having transmittivity of infrared light 10%.

The novelty of our SPV technique is in the detection of the signal from the edge of the QW between an ohmic contact and a side electrode which is made of $25 \text{ \AA} \text{ Al}_2\text{O}_3$ (prevent leakage) and 1000 \AA gold layers on the cleaved surface (Fig. 1a). In the edge SPV (E-SPV) spectroscopy, electron-hole pairs are generated by transitions from the filled valence to the empty conduction band edge states in the depletion-strip (Fig. 1c). The experiments are done in a range of energies for which the electron LLs are empty at the edge and available for optical transition, but are filled in the interior, forbidding optical transition. As a result, the photo-absorption between the quantized states in the depletion-strip occur selectively. After photo-absorption, generated electron-hole pairs can either recombine by emitting photon or relax to their minimum position (Fig. 1c). In our experiment, the second process gives rise to E-SPV signal. The generated E-SPV signal is 100 V at excitation power density 30 nW/cm^2 . Very sensitive unity gain buffer amplifier circuit (Fig. 1a) made of electrometer grade operational amplifier is used to measure the SPV signals. The shield of the input cable is driven by the output of the amplifier to nullify the input cable capacitance, which enable the circuit to measure photovoltage generated from sub femto-coulomb charge. Differential voltage is measured between two such amplifiers, one connected to ohmic contact and the other to side (for E-SPV) or top electrode (for B-SPV).

The E-SPV spectra at selected B values are plotted in Fig. 2. The distinct peaks in the E-SPV spectra are progressively resolved and shift to higher energy with increasing B. However, Zeeman splitting is not resolved indicating that the Zeeman energy is less than the broadening of the peaks.

The B values for E-SPV experiments are selected from two-terminal magnetoresistance (2TMR) plot (Fig. 3a), identified with the filling fractions ν , where $\nu = n_s/(eB/h)$ is defined as the number of filled LLs and eB/h is the density of states (DOS) of a spin-split LL. The 2TMR is measured between two ohmic contacts (Fig. 1a) and it is a combination of Hall (R_H) and longitudinal (R_L) resistances. At the 2TMR plateaus, $R_L = 0$, such that the measured resistance is purely Hall resistance of well defined values h/e^2 with integer filling fraction. At the plateau-to-plateau transitions, R_L goes through a maximum and shows a hump at the beginning of each plateau.

The B-SPV experiment at finite B is discussed in appendix A. The E-SPV and B-SPV spectra at $B = 0$ are compared in Fig. 3b. Blue-shift of the B-SPV spectrum,

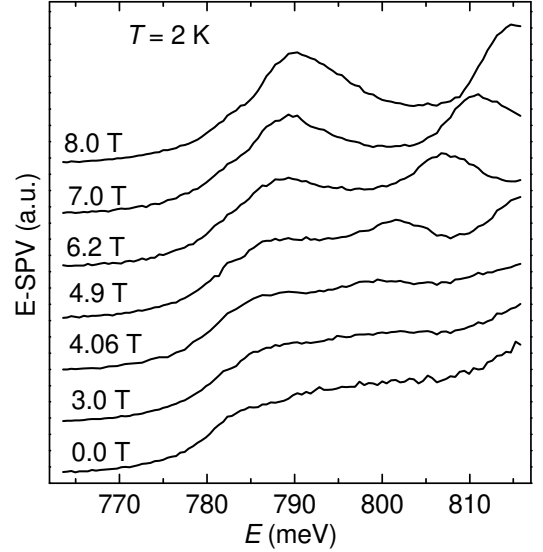


FIG. 2: Plots of the E-SPV spectra at different B fields (measured without passing any external current). The plots are shifted vertically for clarity.

compared to the E-SPV spectrum, results from the band filling of electrons¹⁰. This comparison proves that the edge states are probed distinctively from the states in the interior. The E-SPV spectrum for $B = 0$ rises at an energy characteristic of the band gap of the QW and is flat at higher energies. The SPV signal results from generation of electron-hole pairs by photo-absorption and charge separation. Because of low measurement temperature, excitons do not break into electron-hole pairs¹¹. Therefore, the E-SPV spectrum ($B = 0$) is free from excitonic peak like feature (Fig. 3b). Also, we do not see Franz-Keldysh oscillation in the E-SPV spectrum because of low electric field at the edge. Moreover, the observed E-SPV ($B = 0$) spectrum is less sharper (Figs. 3b & c) than an ideal sample, possibly due to disorder and the edge electric field. In order to determine the band gap energy E_g , the E-SPV spectrum is numerically smoothed and numerical derivative of the smoothed curve is taken (Fig. 3c). The maximum of the derivative is well defined, which gives the band gap energy $E_g = 780.9 \pm 0.3 \text{ meV}$ at temperature 2 K .

The energetics of the edge states from edge spectra (Fig. 2) can be understood in terms of single particle picture in the depletion-strip because of the absence of the electron-electron interaction. Considering constant electric field F along x towards the boundary (Fig. 1a) in the depletion region, single particle Hamiltonian of an electron without the Zeeman energy can be written as

$$H = \frac{1}{2m_e} (\mathbf{p} - e\mathbf{A})^2 + eFx \quad (1)$$

with the Landau gauge of the magnetic vector potential

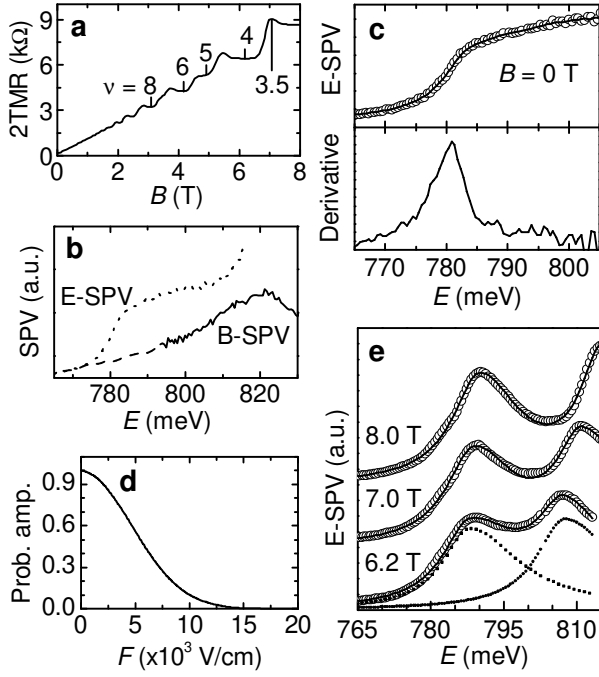


FIG. 3: a) Plot of 2TMR at 1.8 K, filling fraction. b) Comparison of E-SPV and B-SPV at $B = 0$. At the higher energies (792-830 meV), the B-SPV signal is measured by conventional method⁹ at 8 K. c) Upper plot is numerically smoothed E-SPV spectrum (solid line), circles represent data points. Lower plot is derivative of the numerically smoothed spectrum. d) Plot of normalized transition probability amplitude at $B = 8$ T with F considering $m_e = 0.047m_e$, $m_{hh} = 0.173m_e$ and localized wavefunction along x . e) Curves fitted to the E-SPV spectra. Circles represent the numerically smoothed E-SPV spectra and the solid lines are the fitted curves. Dotted lines are two components of the fitted curve for $B = 6.2$ T spectrum.

$A(0; xB; 0)$, where m_e is the electron effective mass and p is the momentum vector. Using Eq.1 the energy $E_{n;k_y}$ for n th LL is deduced¹⁰ as

$$E_{n;k_y} = \left(n + \frac{1}{2}\right) \hbar \omega_c + \frac{F}{B} k_y \frac{1}{2} m_e \frac{F}{B}^2 \quad (2)$$

where $\omega_c = eB/\hbar m_e$ is the cyclotron frequency, k_y is the quantized wave vector along y (boundary). The second and third terms in Eq.2 are respectively linear dispersion and the energy correction introduced by the field F . Solving the Schrödinger equation for heavy hole and using Eq.2, the edge transition energy E_{Tn} from n th hole LL to n th electron LL is deduced as

$$E_{Tn} = E_g + \left(n + \frac{1}{2}\right) \hbar \omega_r + \frac{1}{2} (m_e + m_{hh}) \frac{F}{B}^2 \quad (3)$$

where $\omega_r = eB/\hbar m_r$ is reduced cyclotron frequency, $m_r = m_e m_{hh}/(m_e + m_{hh})$ is reduced mass and m_{hh} is heavy

hole mass. Momentum conservation eliminates the dispersion term in Eq.3. The third term in Eq.3, independent of n , is the electric field (EF) correction to the energy E_{Tn} . If a weak parabolic potential in the depletion-strip is considered, the edge transition energy remains same as in Eq.3, only F increases linearly with x .

The variation of F with x in the depletion-strip of a real sample is not simple. Away from the interface of conducting and depletion strips (along x , Fig. 1c) F becomes larger due to the parabolic and the higher order terms (Taylor expansion) of the edge potential. Therefore, in the depletion-strip the value of F is minimum at the interface of conducting strip and maximum at the boundary of the 2DES. The variation of F in the depletion-strip introduces variation of optical transition probability along x . Due to the field F , the total shift between the centre of masses¹⁰ of electron and hole, having same wave vector k_y , is $(m_e + m_{hh})F/eB^2$. The transition probability includes the overlap integral of electron-hole wave functions and is plotted for a constant field $B = 8$ T with respect to F in Fig. 3d. Since significantly larger fields (F) are present in the depletion-strip near the sample boundary, this region would hardly contribute to the transition between the valence to conduction band edge states according to Fig. 3d. Therefore, we measure the transition energies, in the first approximation, at the minimum electric field region in the depletion-strip, which lies just at the boundary of the conducting-strip. Thus, E-SPV experiment selectively measures the average transition energy near the interface of conducting and depletion strip. The line shape of the E-SPV spectra are asymmetric because of the variation of transition probability with F in the depletion-strip.

Asymmetric Lorentzian curves are fitted to the numerically smoothed E-SPV spectra (Fig. 3e) and the peak positions of the fitted curves give the average edge transition energies E_{T1} and E_{T0} near the interface of conducting and depletion strip. The edge transition energies are plotted in Fig. 4 with B and we clearly see a linear dependence of E_{T1} and E_{T0} on B in the QH regime. More importantly, we verify experimentally the inequality $1/3(E_{T1} - E_g) > (E_{T0} - E_g)$ for a given B , which proves the existence of the EF correction (Eq.3). The observed inequality can not result from band non-parabolicity, which would yield the inequality $1/3(E_{T1} - E_g) < (E_{T0} - E_g)$ as the cyclotron energy would decrease with increasing energy due to the increasing effective mass m_e .

The linear E_{Tn} plots passing through E_g at $B = 0$ is a key finding. The linearity of E_{Tn} in the QH regime implies that the EF correction is either constant or proportional to B . The E_{Tn} plots passing through E_g at $B = 0$ confirms the linear variation of the EF correction with B (Fig. 4). Using Eq.3 and the slopes of the E_{Tn} plots, we obtain cyclotron energy per unit B field as $E_r = \hbar \omega_r/B = 3.15 \pm 0.06$ meV/T and $m_r = (0.037 \pm 0.001)m_e$. Furthermore, we obtain the EF correction per unit B field as $E_{ef} = 0.42 \pm 0.06$ meV/T.

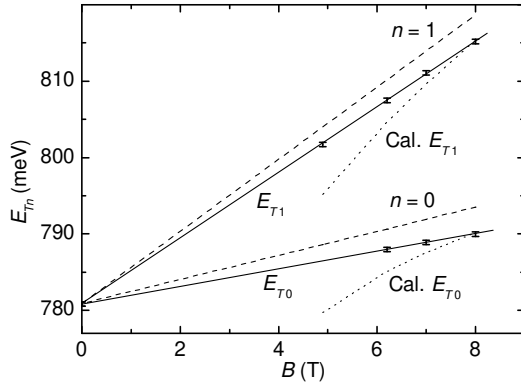


FIG. 4: Plots of the energies E_{T1} and E_{T0} with B . Dashed lines are the bulk transition energies for $n = 0$ and $n = 1$ without EF correction. Dotted lines are the calculated curves for E_{T1} and E_{T0} (Cal. E_{T1} and E_{T0}) considering fixed $F = 5.84 \times 10^3$ V/cm in Eq.3.

From the linearity of the EF correction, we get the most fundamental finding that the average electric field F_{av} at the interface of conducting and depletion strip increases as a power law $B^{3/2}$. The striking consequence of the finding is that the depletion width l_d shrinks with increasing B , since $l_d = b/F_{av}$ and the surface barrier potential ϕ_b ($\phi_b = 250$ meV for InGaAs Ref.¹²) remains constant by the pinning of E_F . From the EF correction, we get an estimate for $F_{av} = 5.8 \times 10^3$ V/cm at $B = 8$ T, using $m_e = 0.047m_e$ Ref.¹³ and $m_{hh} = 0.173m_e$.

For a clear understanding about the EF correction, we plot the bulk transition energies (without the EF correction) $E_g + 1.5\hbar\omega_c$ for $n = 1$ and $E_g + 0.5\hbar\omega_c$ for $n = 0$ in Fig. 4. The red shift of the edge transition energies E_{T1} and E_{T0} due to the EF correction is clearly seen. Furthermore, we plot the calculated curves of E_{T1} and E_{T0} in Fig. 4 using Eq.3 and keeping a constant electric field (hard potential) $F_{av} = 5.84 \times 10^3$ V/cm deduced at $B = 8$ T. The calculated curves deviate much beyond the error bar from the experimental points. Therefore, the linearity in E_{Tn} with B can only be explained by a B dependent electric field $F_{av} / B^{3/2}$ (soft potential).

The dependence $F_{av} / B^{3/2}$ shows that the edge potential is soft i.e. the potential profile at the edge depends on charge redistribution⁶ with B in the conducting-strip because of the counter balance of the local electrostatic and electromagnetic forces. Therefore, the B -dependence of the electric field F_{av} results from a B dependent screening effect in the conducting-strip.

Due to the screening effect, the electron density in the conducting-strip gradually decreases from the bulk value n_s to zero¹⁴ at the interface of conducting and depletion strips. At the interface, application of Gauss's theorem shows that the electric field is continuous. Therefore, the electric field component along x in the conducting-strip near the interface is same as the measured F_{av} in the depletion-strip. Hence, our finding has another con-

sequence, viz., the average velocity of electrons $v_{av} = F_{av}/B$ near the interface increases as a power law $B^{1/2}$. The average velocity of electrons $v_{av} = 7.3 \times 10^6$ cm/s is estimated at 8 T.

Surprisingly, the dependence $v_{av} / B^{1/2}$ is same as the B -dependence of the Landé velocity of electrons $\omega_c l_0 / B^{1/2}$ ($\omega_c l_0 = 2.71 \times 10^7$ cm/s at 8 T), $l_0 = (\hbar/eB)^{1/2}$ is the magnetic length. Single particle quantum mechanical analysis (for example Eq.2) gives the velocity of electrons as F/B . So far there is no theoretical analysis which relates the velocities F/B and $\omega_c l_0$. In reality, the charge redistribution with B at the edge is taking place in such a way that the dependence $F_{av} / B^{3/2}$ (hence $v_{av} / B^{1/2}$) emerges. But the detailed understanding of our results requires a self-consistent calculation including B dependent screening.

We have established that SPV spectroscopy is a unique technique to probe the edge states. As an extension of our experiment, using the E-SPV spectroscopy, the interplay between the Hall current (external) and the chiral current¹⁵ can be probed. Apart from that, our spectroscopic technique has numerous potential applications to probe Fermi liquid to Luttinger liquid transition¹⁶ and the energetics of the Luttinger liquid¹⁷ in fractional QH systems. Using our spectroscopic technique the relaxation process, which generates E-SPV signal, in the edge states can also be studied. Other applications of our SPV technique are discussed in appendix B.

Our experiment displays the general electrodynamics in the quantum mechanical limit i.e. the effect of the B dependent interaction among the mobile electrons in the edge states as the power law dependences of the transverse (Hall) electric field and the electron velocity on B . The observed power-law dependence has to be considered in the theory of the electrostatics and reconstruction of the edge states¹⁴ to understand the electrochemical potential distribution, which is very important in the exact quantization of the Hall resistance in the integer and fractional QH effects.

APPENDIX A

The B-SPV signal is measured with varying B at the excitation energy 815.8 meV (1520 nm) and is plotted in Fig. 5 along with the 2TMR for comparison. The excitation energy 815.8 meV is the closest available energy for the transition from filled valence to empty conduction band LLs at the Fermi energy in the interior. The B-SPV experiment maps the LLs as each LL crosses the Fermi energy E_F . The B-SPV signal is measured by keeping the sample edges covered with aluminum foil. At low magnetic field, we see oscillations in the B-SPV signal (inset of Fig. 5) analogous to the Shubnikov-de Haas oscillations. In the QH regime, sharp peaks appear in the B-SPV signal at even- to odd- plateau to plateau (PP) transitions corresponding to spin-split LLs. The widths and the heights of successive B-SPV peaks increase with

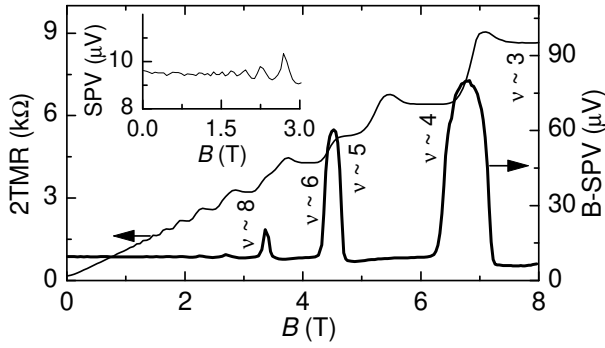


FIG. 5: Plot of B-SPV signal and 2TMR with B . Inset shows the B-SPV oscillations at low B .

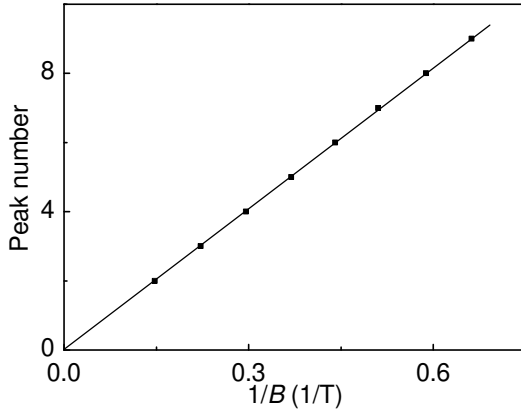


FIG. 6: Plot of B-SPV peak number versus $1/B$.

B due to increase of the density of states ($eB = h$) of the LLs. Similar B-SPV peaks at odd- to even- PP transitions are not observed because the transitions require higher energy due to higher Landau and Zeeman energies, which will be published elsewhere. In addition, sharp rise and fall of the B-SPV peaks are seen.

The unusual shape of the B-SPV peaks in Fig. 5 can be easily understood. In the presence of disorder, degenerate LL broadens into a band of extended states surrounded by localized tail states which are sharply separated by the mobility edges. The electron and hole localized states would be spatially separated; hence overlap integral between electron-hole wave functions is small. As a result, the probability of transition between them is also small. Moreover, the transition probability between localized states and extended states is also negligible because of small overlap integral. The sharp rise and fall of the B-SPV peaks in Fig. 5 are seen because the B-SPV experiment maps the joint-density of extended states. As

a result, we see sudden onset of the optical transition between the extended states as well as sudden fall with increasing B as the mobility edges cross the E_F . Therefore, in the B-SPV experiment, we can measure directly sum of the widths of electron and hole extended states.

Successive B-SPV peaks in Fig. 5 are assigned integer numbers in increasing order from higher to lower B , and corresponding B values of the peaks are determined. The peak number versus $1/B$ plot (Fig. 6) is linear, having a slope of $n_s h = 2e$. The slope of this plot provides an estimate of the electron density $n_s = (6 \pm 0.03) \times 10^{11} \text{ cm}^{-2}$.

The B-SPV and E-SPV spectra at $B = 0$ are compared in Fig. 3b. The energy of transition $E_{TF} = 822 \text{ meV}$ from valence band to empty conduction band states near the E_F is determined from the peak in the B-SPV spectrum which is shifted by $n_s h^2 = m_r$ in comparison to E_g . Using the values of E_g , n_s and m_r , the transition energy E_{TF} is estimated as $823.6 \pm 1.7 \text{ meV}$, which matches reasonably. The B-SPV spectrum in the QH regime and the consequences of the results will be published elsewhere.

APPENDIX B

The B-SPV experiments are done in weakly invasive manner such that the generated B-SPV signal ($\sim 100 \text{ V}$) is much less than the surface barrier potential ($\sim 300 \text{ mV}$ for InP) with low excitation power density, $\sim 1 \text{ W/cm}^2$ after attenuation in the top electrode. The B-SPV experiments require lower excitation power density ($\sim 1 \text{ W/cm}^2$) compared to that used in the conventional transmission experiments¹⁸ by about a factor of 1000 and in the inelastic light scattering experiments¹⁹ by about a factor of 100. Very weak perturbation of the system enables us to measure the widths of the joint density of states directly (Fig. 5). Therefore, in the quantum Hall system the B-SPV experiment can be used to study the quantum criticality²⁰, in that the nature of the dependence of the width of the extended states with temperature is studied. Using B-SPV experiment, the manybody excited states²¹ above the Fermi energy in the fractional quantum Hall system can also be studied.

ACKNOWLEDGMENTS

We gratefully acknowledge helpful discussions with D. Dhar, K. L. Narasimhan, B. Bansal and S. Bhattacharya. We thank R. Bhat for providing sample, E. L. Ivchenko for useful comments, A. P. Shah for help in device preparation, S. Ghosh and J. Bhattacharya for conventional B-SPV measurement used in Fig. 3b.

¹ B. I. Halperin, Phys. Rev. B 25, 2185 (1982).

² M. Böttiker, Phys. Rev. B 38, 9375 (1988).

- ³ A. Lorke, J. P. Kotthaus, J. H. English, A. C. Gossard, Phys. Rev. B 53, 1054 (1996).
- ⁴ K. K. Choi, D. C. Tsui, K. A.avi, Appl. Phys. Lett. 50, 110 (1987).
- ⁵ K. Arai, S. Hashimoto, K. O to, K. M urase, Phys. Rev. B 68, 165347 (2003).
- ⁶ K. Guven and R. R. Gerhardts Phys. Rev. B 67, 115327 (2003).
- ⁷ D. J. Thouless Phys. Rev. Lett. 71, 1879 (1993).
- ⁸ W. Kang, H. L. Stormer, L. N. Pfei er, K. W. Baldwin and K W. West, Nature 403, 59 (2000).
- ⁹ S. Datta, S. Ghosh, B. M. A rora, Rev. Sci. Inst. 72, 177 (2001).
- ¹⁰ J. H. Davies, The Physics of Low-D im ensional Sem icon-ductors (Cam bridge University Press 1998).
- ¹¹ D. Tari, M. D. G iorgi, R. C ingolani, E. Foti and C. Cori-asso, J. App. Phys. 97, 043705 (2005)
- ¹² P. Bhattacharya Ed., Properties of Lattice-M atched and Strained Indium Gallium Arsenide EM IS D ataview s Series No. 8 (An INSPEC Publication, 1993).
- ¹³ M. Sugawara, N. Okazaki, T. Fujii, S. Yam azaki, Phys. Rev. B 48, 8102 (1993).
- ¹⁴ D. B. Chklovskii, B. I. Shklovskii, L. I. Glazm an, Phys. Rev. B 46, 4026 (1992).
- ¹⁵ K. Shizuya, Phys. Rev. Lett. 73, 2907 (1994).
- ¹⁶ M. H ilke, D. C. Tsui, M. G rayson, L. N. Pfei er and K. W. West, Phys. Rev. Lett. 87, 186806 (2001).
- ¹⁷ X. G. W en, Phys. Rev. B 41, 12838 (1990).
- ¹⁸ E. H. A ifer, B. B. G oldberg, D. A. B roido, Phys. Rev. Lett. 76, 680 (1996).
- ¹⁹ M. K ang, A. P inczuk, B. S. Dennis, M. A. Eriksson, L. N. Pfei er, and K. W. West, Rev. Lett. 84, 546 (2000).
- ²⁰ A. M. M. P niskanen, Phys. Rev. Lett. 61, 1297 (1988).
- ²¹ I. D ujpne, et. al., Phys. Rev. Lett. 90, 036803 (2003).